PRECIPITATION HARDENING AND STRAIN LOCALIZATION: INSTABILITIES INDUCED BY GEOMETRICAL SHEARING OR BY CHEMICAL REVERSION

Y. Bréchet and F. Louchet
Laboratoire de Thermodynamique et Physico-Chimie Métallurgiques, E.N.S.E.E.G, BP.75,
38402 Saint Martin d'Heres, France

ABSTRACT Strain localization and instabilities are studied in two extreme cases: the first one deals with the competition between precipitate shearing and coarsening, the second between strain induced reversion of ordered precipitates and reprecipitation. A particular emphasis is laid on the problem of spatial coupling due to solute diffusion. It is shown that this spatial coupling can lead to strain localization, with a characteristic wavelength which depends on the imposed strain rate and the characteristics of the precipitation (volume fraction, radius, antiphase boundary energy, ...).

I- INTRODUCTION

-Plastic instabilities exhibited by some materials under some straining conditions can be described from two closely related and complementary viewpoints: the temporal aspect of instabilities appears for example on the stress-strain curves (as serrations in the Portevin le Châtelier effect or as yield points followed by a plateau as in the Piobert-Lüders effect for instance) -The spatial aspect appears as a strain localization: some regions of the material deform at a much larger rate than others, and can be either stationnary or propagating. The description of the temporal aspect must take into account the stiffness of the testing machine; this intricate problem will not be examined here. The spatial aspect of strain localization is more closely related to the physical properties of the material itself, and will be our main concern here.
-The presence of shearable precipitates introduced for structural hardening purposes is well known to lead to a strong strain localization (1,2). -Although this effect can be easily understood qualitatively, the spatial aspects, and in particular the derivation of the lengthscale of strain localization, have not been explained up to now. The key of this problem lies in the description of the spatial coupling between neighbouring regions of the crystal which behave in a different way. This coupling can arise either from dislocation interactions or spreading (cross-slip or climb), from diffusion of heat produced by plastic deformation (for instance adiabatic shearing of Nb at low temperatures (3)), or from solute diffusion, which couples the state of precipitation and the related structural hardening in different regions of the sample.
Since it involves long range interactions the coupling through dislocations is an intricate problem although in some cases it can be treated as a diffusion-like problem (4,5,6). The thermal or solute coupling being more local are more likely to be correctly described through diffusion equations. In this paper we will focus our attention only on the solute coupling.
-For the sake of simplicity, we shall make the following assumptions:
1-We shall consider the case of a single crystal in single slip conditions, in particular in order to get rid of strain hardening.
2-The precipitates are assumed to be shearable, coherent and ordered.
The model will then be set up in terms of the following parameters: volume fraction and radius of precipitates, antiphase boundary energy, free enthalpy of precipitation, strain rate $\dot{\varepsilon}$,...The critical stress σ_c for overcoming the precipitates has been already computed in the case of shearable precipitates by various authors (7,8,9). It can be written as:

$$\sigma_c = \sigma_o \frac{R^{3/2}}{\ell b^{1/2}} \quad (1)$$

where ℓ is the precipitate spacing in the slip plane, R the average radius of the intersection of the slip plane with the precipitates, b the Burgers vector, and σ_o a stress-like coefficient which is given by:

$$\sigma_o = \frac{K_o \gamma^{3/2}}{b^{1/2} \Gamma^{1/2}} \quad (2)$$

where γ is the antiphase energy and Γ the dislocations line tension.

In the following, we shall derive the time (or strain) evolution of the critical stress σ_c, look for the steady states, and see whether they are stable or not. For this purpose, we shall examine two extreme cases: the first one deals with geometrical shearing of precipitates by dislocations (softening term) competing with precipitate coarsening (hardening term), and is likely to be found in the case of large but shearable precipitates. The second one deals with strain induced reversion due to shearing by dislocation, softening term competing with reprecipitation (hardening term), which is more likely to occur in the case of small ordered precipitates with a large antiphase boundary energy, at the very beginning of precipitation stage.

II- COMPETITION BETWEEN SHEARING AND COARSENING

-When an ordered precipitate is sheared by a superdislocation, the surface to be sheared by the next one in the same plane is reduced, i.e. the average apparent radius of the precipitate becomes smaller (fig.1). The resulting softening comes from the reduction of the average "effective" radius R, and not from the separation l between precipitates, which remains constant. One must keep in mind that R and l are not related to one another through a relation involving the volume fraction f, since R is related to a surface to be sheared, and not to a precipitate volume.
-This radius reduction competes with precipitate coarsening, which changes both the spacing and the average size of precipitates, the volume fraction being roughly constant (Oswald ripening).

II-1- Homogeneous problem

The softening which results from an effective radius reduction dR can be written, from eq.1:

$$d\sigma_c = \frac{3}{2}\frac{\sigma_o^{2/3}\sigma_c^{1/3}}{l^{2/3}b^{1/3}}dR \qquad (3)$$

We shall now estimate the effective radius reduction dR coming from shearing at a rate $\dot{\varepsilon}$ during dt: the number of dislocations shearing the precipitate during dt is:

$$\rho v dt.2(lf^{1/2})$$

Each of them will reduce the area by 2bR (10).
The resulting area reduction is then:

$$dS = 2\pi R dR = -\rho v dt.2(lf^{1/2}).\ 2bR \qquad (4)$$

and then, using Orowan's equation:

$$\dot{R} = \frac{-2}{\pi} f^{1/2} l \dot{\varepsilon} \qquad (5)$$

The rate of evolution of σ_c coming from this shearing process is:

$$\dot{\sigma}_c\ (\text{shearing}) = \frac{-3}{\pi}\frac{\sigma_o^{2/3}\sigma_c^{1/3}}{l^{2/3}b^{1/3}} f^{1/2} l \dot{\varepsilon} \qquad (6)$$

If this mechanism was the only one to operate, we should observe a complete softening.

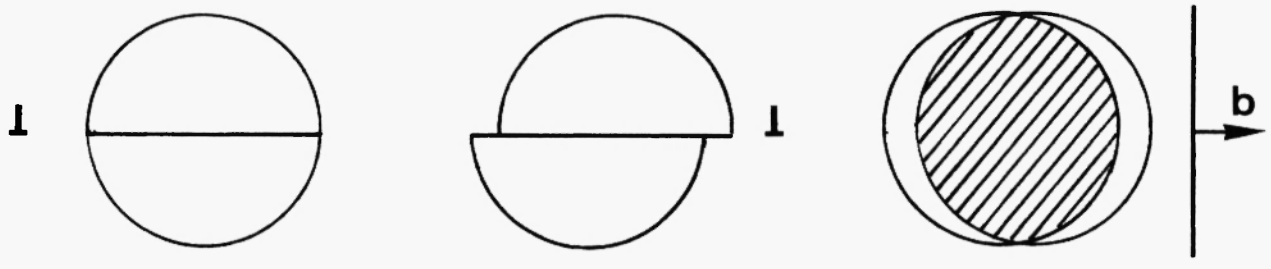

Fig. 1 : Shearing of an ordered precipitate by a dislocation leaving behind it an antiphase boundary (hatched region)

The coarsening kinetics will be now modelled in the simplest way, i.e. using the steady state of Lifschitz Slyozov Wagner (LSW) theory, (11,12), assuming that the evolution of the effective radius R follows the same law as that of the average radius <R>. The LSW equation is:

$$\dot{\langle R\rangle} = \frac{KD}{\langle R\rangle^2} \tag{7}$$

where D is the diffusion coefficient of solute atom, and K a constant which depends on the interfacial energy and is given by:

$$K = \frac{8}{27}\frac{\gamma_S \Omega c}{kT} \tag{8}$$

The resulting rate evolution of σ_c is then:

$$\dot{\sigma}_c \text{ (coarsening)} = \frac{1}{2}\,\frac{\sigma_o^6}{\sigma_c^5}\,\frac{f^3}{b^3}\,KD \tag{9}$$

The overall evolution of σ_c resulting from the competition of the two phenomena results from adding the contributions given by equations.(6) and (9):

$$\frac{\dot{\sigma}_c}{\sigma_o} = \frac{-3}{\pi}\left(\frac{\ell}{b}\right)^{1/3} f^{1/2}\left(\frac{\sigma_c}{\sigma_o}\right)^{1/3}\dot{\varepsilon} + \frac{1}{2} f^3 \frac{KD}{b^3}\,\frac{1}{(\sigma_c/\sigma_o)^5} \tag{10}$$

In a $\frac{\dot{\sigma}_c}{\sigma_o}$ vs $\frac{\sigma_c}{\sigma_o}$ plot (fig.2), one can see that there is a stable attractor given by:

$$\left(\frac{\sigma_c}{\sigma_o}\right)^* = \left[\frac{\pi}{6}\,\frac{KD}{b^3}\,\frac{1}{\dot{\varepsilon}}\,f^{5/2}\left(\frac{\ell}{b}\right)^{-1/3}\right]^{3/16} \tag{11}$$

In order to see whether we have hardening or softening, it is useful to compare the initial value of σ_c and the steady state one. Using equations (1) and (11), and noticing for the sake of simplicity 3/16 ~1/5 and 1/2>>1/15 we find that softening will occur if:

$$\left(\frac{\ell}{b}\right)^{5/2} f^{25/2} > \frac{\pi}{6}\left(\frac{KD}{b^3\dot{\varepsilon}}\right) \tag{12}$$

where it must be noticed that the diffusion coefficient D may depend on the plastic-induced vacancy production as (13):

$$D = D_o + \alpha\,\dot{\varepsilon} \tag{13}$$

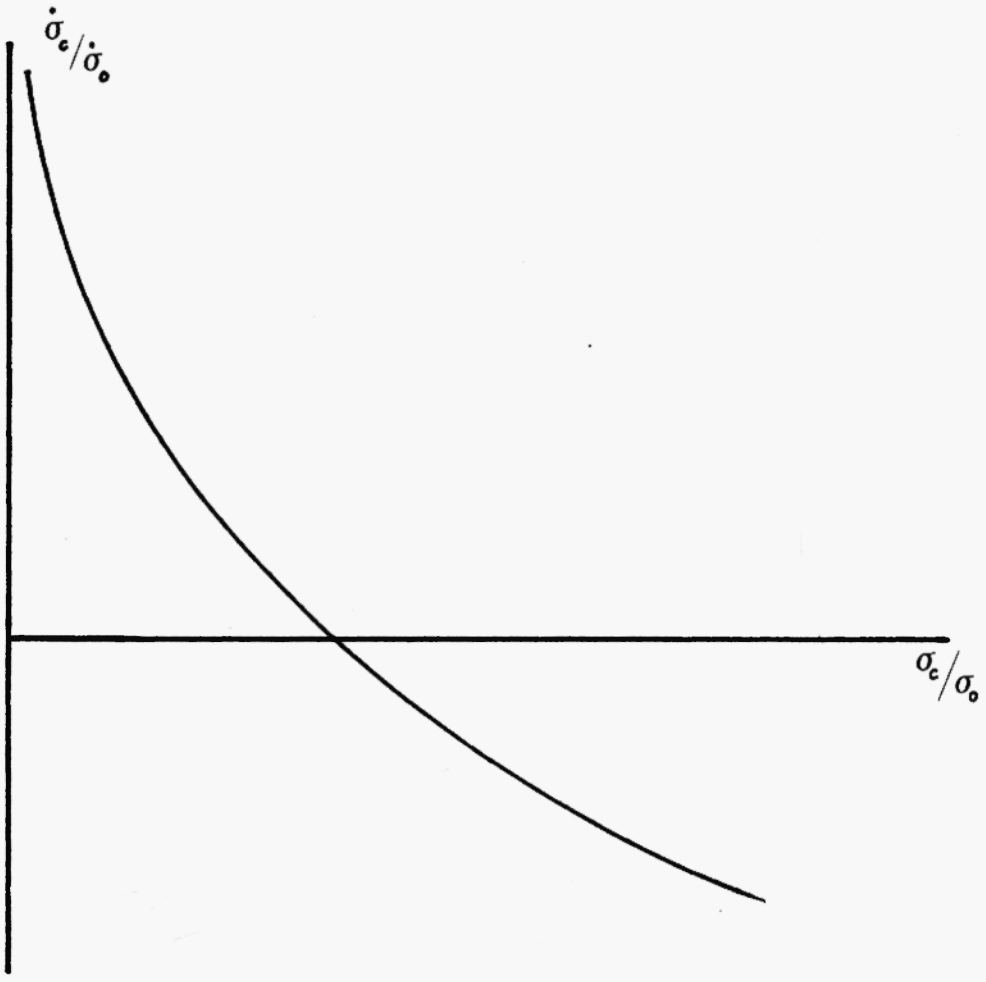

Fig. 2 : Rate of evolution of the critical stress σ_c : case of competition between shearing and coarsening

There is a critical value of $\dot{\varepsilon}$ given by:

$$\dot{\varepsilon} = \frac{D_0}{\frac{6}{\pi}\frac{b^3}{\bar{K}}\left(\frac{\ell}{b}\right)^{5/2} f^{25/2-\alpha}} \tag{14}$$

above which shearing dominates coarsening, and therefore results in a softening.

II-2- Spatial coupling

In order to investigate the stability of the previous homogeneous steady state versus spatial fluctuations, one has to take into account the spatial coupling resulting from solute diffusion between neighbouring regions which have different average precipitate sizes, i.e. different solute supersaturations.

Regions where precipitates are small exhibit a higher supersaturation, and this will result in a solute flux towards regions with lower supersaturations (i.e. larger precipitates) which will then grow faster. This type of instability is inherent to coarsening processes and can occur without the help of plasticity. A spectacular example is found in geology with the "greedy giants" (14,15). The additional effect of plasticity is to introduce an anisotropic diffusion tensor through eq. (13). The normal to the slip planes becomes therefore a particular direction, and the effect of plasticity is to introduce a "texture" in the instability, which otherwise would be isotropic.

The coarsening of a given precipitate results from both the short range interaction between this precipitate and its nearest neighbours (roughly at a distance L), and an interaction at a longer range between regions exhibiting different average radii of precipitates. The first coupling is accounted for by the LSW theory. The additional coupling we are looking for results from the second type of interaction. The volume increase of the precipitate resulting from the flux due to this latter term is:

$$4\pi R^2 \frac{dR}{dt} = - \frac{D\pi R^2}{C_p} [(\nabla c)_{x=-L/2} - (\nabla c)_{x=+L/2}] \cong \frac{\pi R^2}{C_p} LD\,(\nabla^2 c) \qquad (15)$$

Remembering that the supersaturation is given by the Gibbs-Thomson equation:

$$c - c_\infty = \frac{\beta}{R} \qquad (16)$$

with $\beta = \frac{27\,K}{8}$, from which $\nabla^2 c$ can be derived as :

$$\nabla^2 c \cong - \frac{B}{R^2} \nabla^2 R \qquad (17)$$

where the 2d order term in $(\nabla R)^2$ has been neglected. From (15) and (17) the evolution rate of the radius is then:

$$\dot{R} = - \frac{\beta LD}{4R^2 c_p} \frac{d^2R}{dx^2} \qquad (18)$$

From eqs. (1) and (18), the additional contribution to σc due to the coupling mechanism if finally given by:

$$\dot{\sigma}_c\,(\text{coupling}) = - \frac{1}{4} \left(\frac{\sigma o}{\sigma_c}\right)^4 \left(\frac{f}{b}\right)^2 \frac{\beta LD}{c_p} \frac{d^2\sigma c}{dx^2} \qquad (19)$$

It results from eqs. (10) and (19) that the evolution equation for the critical stress σc is:

$$\frac{\dot{\sigma c}}{\sigma o} = - \frac{3}{\pi} \left(\frac{\ell}{b}\right)^3 f^{1/2} \left(\frac{\sigma c}{\sigma o}\right)^{1/3} \dot{\varepsilon} + \frac{1}{2} f^3 \frac{KD}{b^3} \frac{1}{(\sigma c/\sigma o)^5} - \frac{1}{4} \frac{\beta LD}{(\sigma c/\sigma o)^4 c_p} \left(\frac{f}{b}\right)^2 \frac{d}{dx^2} \left(\frac{\sigma c}{\sigma o}\right) \qquad (20)$$

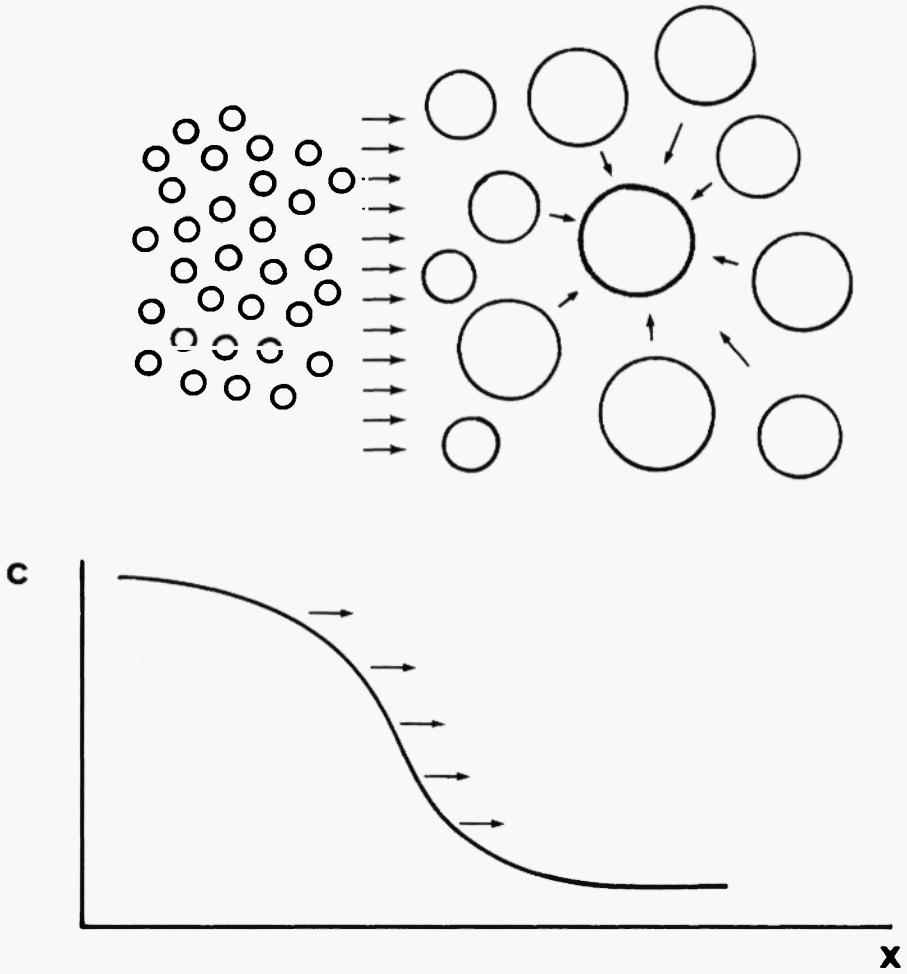

Fig. 3 : Solute gradients associated with a gradient in average size of precipitates

II-3- Stability analysis

We shall look now at the evolution of a small sinusoidal perturbation in space with a wave vector q around the homogeneous steady state given by eq. (11). A standard linear stability analysis (16) leads to an evolution in exp (ω(q)t) where ω (q) is approximately given by:

$$\omega(q) \cong \frac{1}{4c_p} \frac{\beta L D}{(\sigma c^*/\sigma o)^4} \left(\frac{f}{b}\right)^2 q^2 - \frac{16}{3} \left(\frac{\rho}{b}\right)^{3/8} f^{3/16} \varepsilon^{9/8} \left(\frac{b^3}{KD}\right)^{1/8} \qquad (21)$$

and schematically shown in fig.4. The most important result is that any perturbation with a wave vector larger than q_c is unstable, and that the larger is q, the larger is the associated amplification factor ω(q). Practically it means that in presence of both shearing and coupling through solute diffusion, the homogeneous solution is unstable, i.e. strain localization has to occur, but no particular length scale is selected. This means that the distance between neighbour slip bands will be scattered at

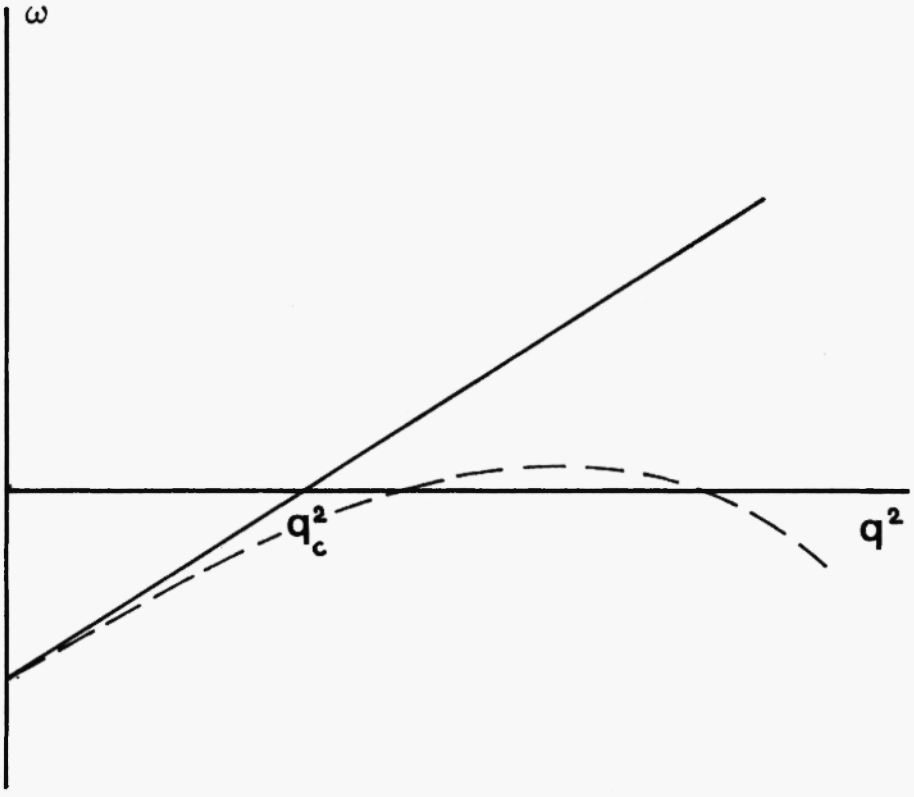

Fig. 4 : Amplification factor $\omega(q)$ of a sinusoidal perturbation of wave vector q : case of competition between shearing and coarsening

full line : classical diffusion equation
dashed line : generalised Cahn Hilliard equation

least between L (which is the limit of validity of our continuum approach) and $2\pi/q_c$. This is to say that considering a given slip band, one has to find another one within a distance less than $2\pi/q_c$, with (after some algebra):

$$q_c^2 \equiv \frac{4}{b^2}\left(\frac{b^3\dot{\varepsilon}}{KD}\right)^{3/8} f^{1/24} \left(\frac{b}{L}\right)^{15/8} \qquad (22)$$

III- COMPETITION BETWEEN STRAIN-INDUCED REVERSION AND REPRECIPITATION

The other extreme case is that where precipitates become unstable through strain induced accumulation of antiphase boundaries (17). In this case, the related softening arises from an increase in the average separation ℓ of precipitates in the slip plane, the radii of the remaining precipitates being constant. Now, ℓ and R are related to each other through the volume fraction f, but f varies. The increase of solute content due to precipitate dissolution increases the precipitation rate with which it is competing.

III-1- Homogeneous problem

The evolution rate of σc can be expressed in terms of $\dot{\ell}$, which itself is related to the evolution rate of the number n of precipitates per unit volume:

$$\dot{\sigma c} = \sigma o \frac{R^{5/2}\,\ell}{b^{1/2}} \frac{2}{3} \pi \dot{n} \tag{23}$$

where n results from a balance between shear-induced dissolution and reprecipitation

The **dissolution** criterion is taken from (17) as:

$$R = R_c(\varepsilon) = R_{co} \frac{1 + \frac{\pi\varepsilon}{8}}{1 - \frac{\varepsilon\gamma a}{b\gamma v}} \tag{24}$$

which is to say that the increase of volume energy due to APB accumulation in the precipitate drives the critical radius Rc(ε) for reversion to a value larger than R. The reversion kinetics are approximated by;

$$dn = -n \frac{dt}{\theta} \tag{25}$$

where θ is a characteristic time for precipitate dissolution, and can be estimated by:

$$\theta = \frac{\varepsilon}{\dot{\varepsilon}} \tag{26}$$

ε being related to R through eq. (24).

Assuming that we are at the very beginning of nucleation, R can be expressed as:

$$R = R_{co}(1 + \xi) \tag{27}$$

where $\xi << 1$.
From eqs. (24),(25),(26),(27) the reverson kinetics becomes:

$$\dot{n} = -\dot{\varepsilon} \frac{\frac{\pi}{8} + \frac{\gamma}{b\gamma_v}}{\xi} n \tag{28}$$

The **precipitation** from the solid solution is classically given by (18):

$$\dot{n} = \dot{n}\,o \exp\left(-\frac{\Delta G^*}{kT}\right) \tag{29}$$

where $\Delta G^* = \frac{16}{3}\pi \frac{\gamma_s^3}{\gamma_v^2}$ (30)

The supersaturation dependence of γ_v can be written:

$$\gamma_v = \gamma_o(c-c_{eq}) \tag{31}$$

with $\gamma_o = \frac{1}{2}\cdot(c_p-c_{eq})\left(\frac{\partial^2 G}{\partial C^2}\right) c=c_{eq}$ (32)

The solute concentration can itself be written as:

$$c = c_o - \frac{4}{3}\pi R^3 n c_p \tag{33}$$

The evolution rate of n resulting from both precipitation and shear-induced reversion is then:

$$\dot{n} = \dot{n}_o \exp\left[- \frac{16\pi}{3kT} \frac{\gamma_s^2}{\gamma_o^3} \frac{1}{\left(\frac{4}{3}\pi R^3 c_p\right)^3 (n_c - n)^3} \right] - \frac{\dot{\varepsilon}}{\xi}\left[\frac{\pi}{8} + \frac{\gamma_a}{b\gamma_o \frac{4}{3}\pi R^3 c_p}\left(\frac{n}{n_c - n}\right)\right] \tag{34}$$

where: $n_c = \frac{c_o - c_{eq}}{\frac{4}{3}\pi R^3}$ (35)

The evolution of σc can be derived directly from eqs. (23), (34) and (35).

$$\frac{\dot{\sigma}}{\sigma_{..}} = \frac{2\pi R^4}{3b} \frac{1}{\left(\frac{\sigma}{\sigma_o}\right)} \left[\dot{n}_o \exp\left(\frac{-16\pi}{3kT} \frac{\gamma_s^2}{\gamma_o^3} \frac{1}{\left(\frac{4}{3}\pi R^3 c_p\right)^3 \left[n_c - \frac{3b}{4\pi R^4}\left(\frac{\sigma}{\sigma_o}\right)^2 \right]} \right) - \frac{\dot{\varepsilon}}{\xi}\left(\frac{\pi}{8} + \frac{\gamma_a}{b\gamma_o \frac{4}{3}\pi R^3 c_p} \frac{1}{\frac{4\pi n_c R^4}{3b\left(\frac{\sigma}{\sigma_o}\right)^2} - 1} \right) \right] \tag{36}$$

$\frac{\dot{\sigma}_c}{\sigma_o}$ can be plotted versus $\frac{\sigma_c}{\sigma_o}$ as in §II-2 (Fig.5).

This plot shows that, once more, we have a *stable attractor* $\frac{\sigma_c^*}{\sigma_o}$. Depending on the starting point on

the evolution curve of Fig.5, we can have either softening or hardening. If nucleation is almost completed in the predeformed state, the reversion will be dominant and will lead to softening. On the contrary, if we start with a highly supersaturated solution, nucleation will dominate, and result in hardening. In the former case, it is worth noting that the softening will increase when the strain rate $\dot{\varepsilon}$ is increased, or when the diffusion coefficient is decreased.

III-2- Spatial coupling

For the sake of simplicity, we shall consider in the following the evolution equation for n and not for $\frac{\sigma}{\sigma_0}$. In the case of coarsening discussed in §II, the supersaturation, in both the homogeneous and the inhomogeneous cases, is small compared to the nominal concentration c_0, which allowed us to neglect the spatial variations of c_0. Here we are considering a reversion process, where a large amount of solute is driven back into the solid solution. We therefore need to study now

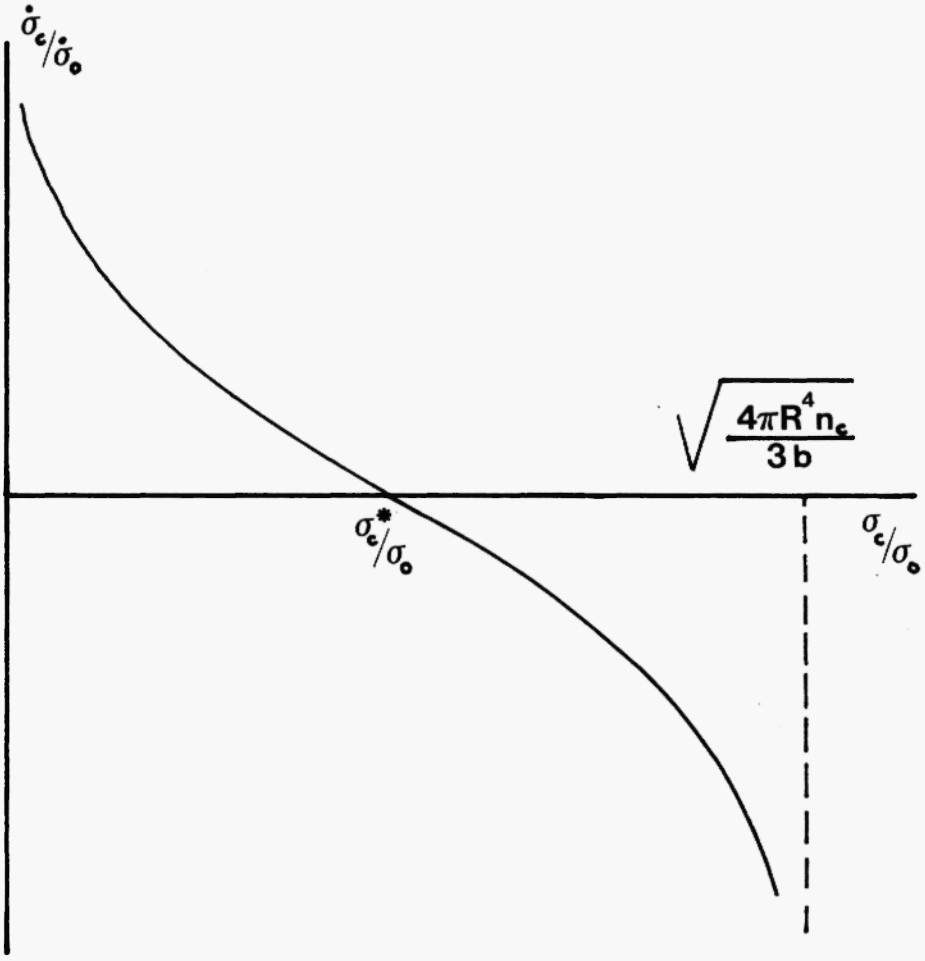

Fig. 5: Rate of evolution of the critical stress σ_c : case of competition between strain induced dissolution and reprecipitation

the coupled evolution of n *and* c_o. In the regions of highly supersaturated solution, nucleation is a local process, i.e. it does not need long range diffusion. However this does not prevent a long range diffusion of atoms in solid solution, which results in a spatial coupling acting on the evolution rate of c_o. This evolution rate for c_o is dominated by the diffusion of solute atoms in solid solution :

$$\dot{c}_o = D\frac{\partial^2 c}{\partial x^2} \tag{37}$$

which can be written using eq. (33) :

$$\dot{c}_o = D\frac{\partial^2 c_o}{\partial x^2} - \frac{4}{3}\pi R^3 c_p D\frac{\partial^2 n}{\partial x^2} \tag{38}$$

III-3- Stability analysis

Eq. (34) is of the type :

$$\dot{n} = \varphi(n, c_o) \tag{39}$$

and then eqs. (38) and (39) form an autonomous system of partial differential equations. The linear stability of the associated spatially homogeneous steady state solution can be investigated by the standard method (16): it is governed by the sign of the real parts of the eigenvalues of the associated Jacobian matrix. Its secular determinant is:

$$\begin{vmatrix} \frac{\partial\varphi}{\partial n} - \omega(q) & \frac{\partial\varphi}{\partial c_o} \\ \frac{4}{3}\pi R^3 c_p q^2 D & -Dq^2 - \omega(q) \end{vmatrix} = 0 \tag{40}$$

where it can be noticed from eqs. (34) and (35) that $\frac{\partial\varphi}{\partial\sigma_{II}} < 0$ and $\frac{\partial\varphi}{\partial c_o} > 0$.

The amplification factors $\omega(q)$ of a perturbation of wave vector q are solutions of eq.(40):

$$\omega^2 + \omega\left(Dq^2 - \frac{\partial\varphi}{\partial n}\right) + Dq^2\left(-\frac{\partial\varphi}{\partial c_o}\frac{4}{3}\pi R^3 c_p - \frac{\partial\varphi}{\partial n}\right) = 0 \tag{41}$$

The sum of the two roots is always negative. The condition for instability will be therefore that the two roots are real, and one of them positive. The instability condition can then be written:

$$-\frac{\partial\varphi}{\partial c_o}\frac{4}{3}\pi R^3 c_p - \frac{\partial\varphi}{\partial n} < 0 \tag{42}$$

In this case:

$$\omega(q) = \frac{1}{2}\left\{\left(\frac{\partial\varphi}{\partial n} - Dq^2\right) + \sqrt{\left(Dq^2 - \frac{\partial\varphi}{\partial n}\right)^2 + 4\left(\frac{\partial\varphi}{\partial c_o}4\pi R^3 c_p + \frac{\partial\varphi}{\partial n}\right)Dq^2}\right\} \quad (43)$$

which is plotted in Fig.6.
As in §II, no characteristic wave length is selected, any one between zero and infinity being unstable.

IV- DISCUSSION AND CONCLUSIONS

The competition between geometrical shearing and coarsening and between reversion and nucleation can be illustrated in Al-Li alloys in Figs. 7 and 8. Although these experiments were performed in cyclic straining, similar results could be expected in monotonous testing, if the failure of the specimen did not prevent from reaching easily the steady state. In addition, these alloys exhibit a

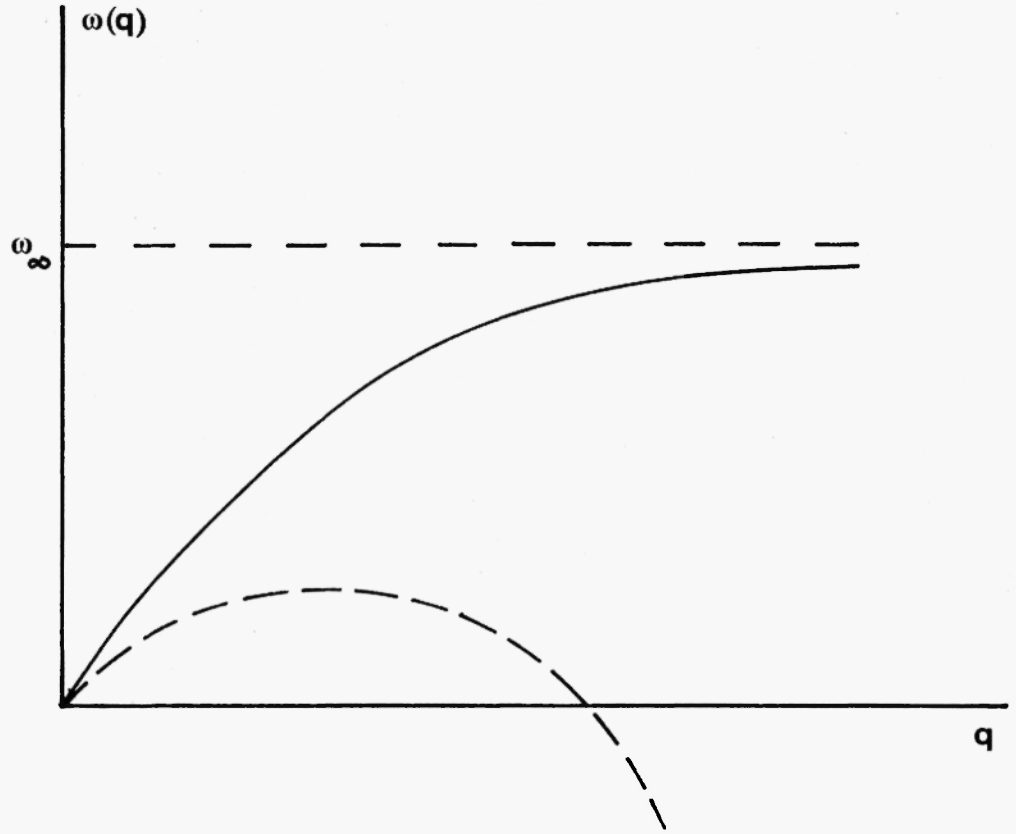

Fig. 6 : Amplification factor ω(q) of a sinusoidal perturbation of wave vector q : case of competition between shear induced dissolution and reprecipitation :

full line : classical diffusion equation
dashed line : generalized Cahn Hilliard equation

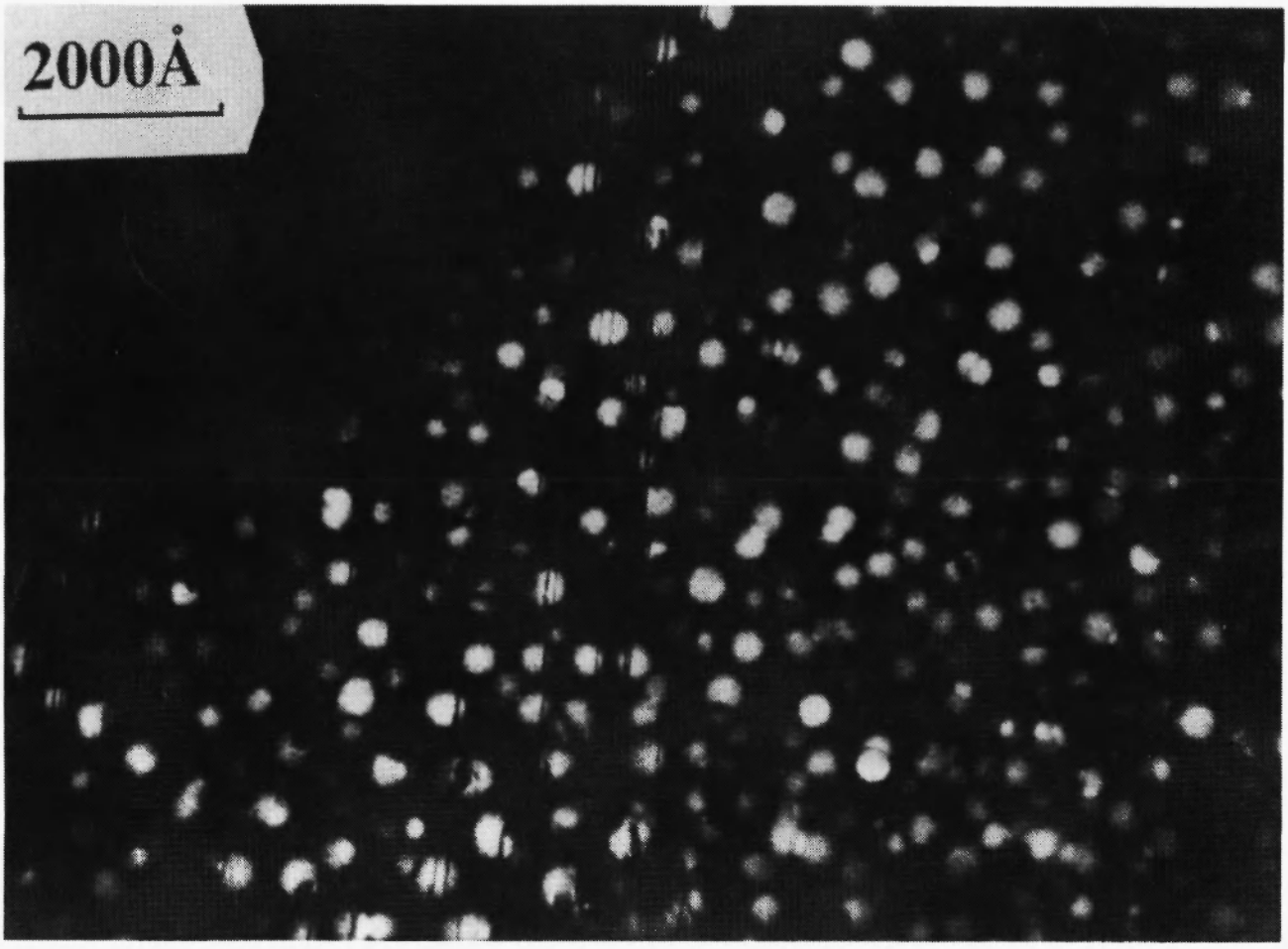

Fig. 7: Al 2.5 % Li alloys aged 45 hours at 195°C, fatigued in torsion ($\Delta\varepsilon_t$ = 0.5 %) : sheared δ' precipitates after fatigue, superallatice dark field [110], zone axis [110]

very low hardening and one dominant slip plane, which brings the situation closer to the academic case examined here. The problem of spatial coupling we have studied is strongly reminiscent of that of spinodal decomposition (19, 20) which involves a "negative diffusion coefficient". The classical diffusion equation in our case as well as in spinodal decomposition fails in selecting a dominant instability wavelength. The physical reason for this failure is that such a treatment neglects the "interfacial energies" arising from the strong solute gradients involved in short wavelength fluctuations. These large q fluctuations are actually stabilized by this interfacial energy term introduced in the case of spinodal decomposition by Cahn, Hilliard and Hillert (19, 20, 21). Similarly, we can expect here the same kind of stabilization, and therefore a selected wavelength (dotted lines in Figs. 4 and 6). A strong qualitative difference arises then between the two cases: in the first case of geometrical shearing and coarsening a strong interfacial energy effect would kill all the instabilities, whereas this will never happen in the second case of reversion vs nucleation competition. This approach has obviously an academic character for several reasons. First it is well known (22, 23) that it is quite artificial to separate nucleation from coarsening. Second, spatial coupling does not arise only from solute diffusion, but also from thermal diffusion or (and) dislocation interactions and spreading. In addition, work hardening which has been neglected in this

approach is very likely to act as a stabilizing factor, especially in the case of multislip.
- However, this approach allows in a simple case to evidence the unstabilizing factors in alloys with shearable precipitates, and to introduce explicitely a simple kind of spatial coupling from which arise the characteristic lengths of strain localization.

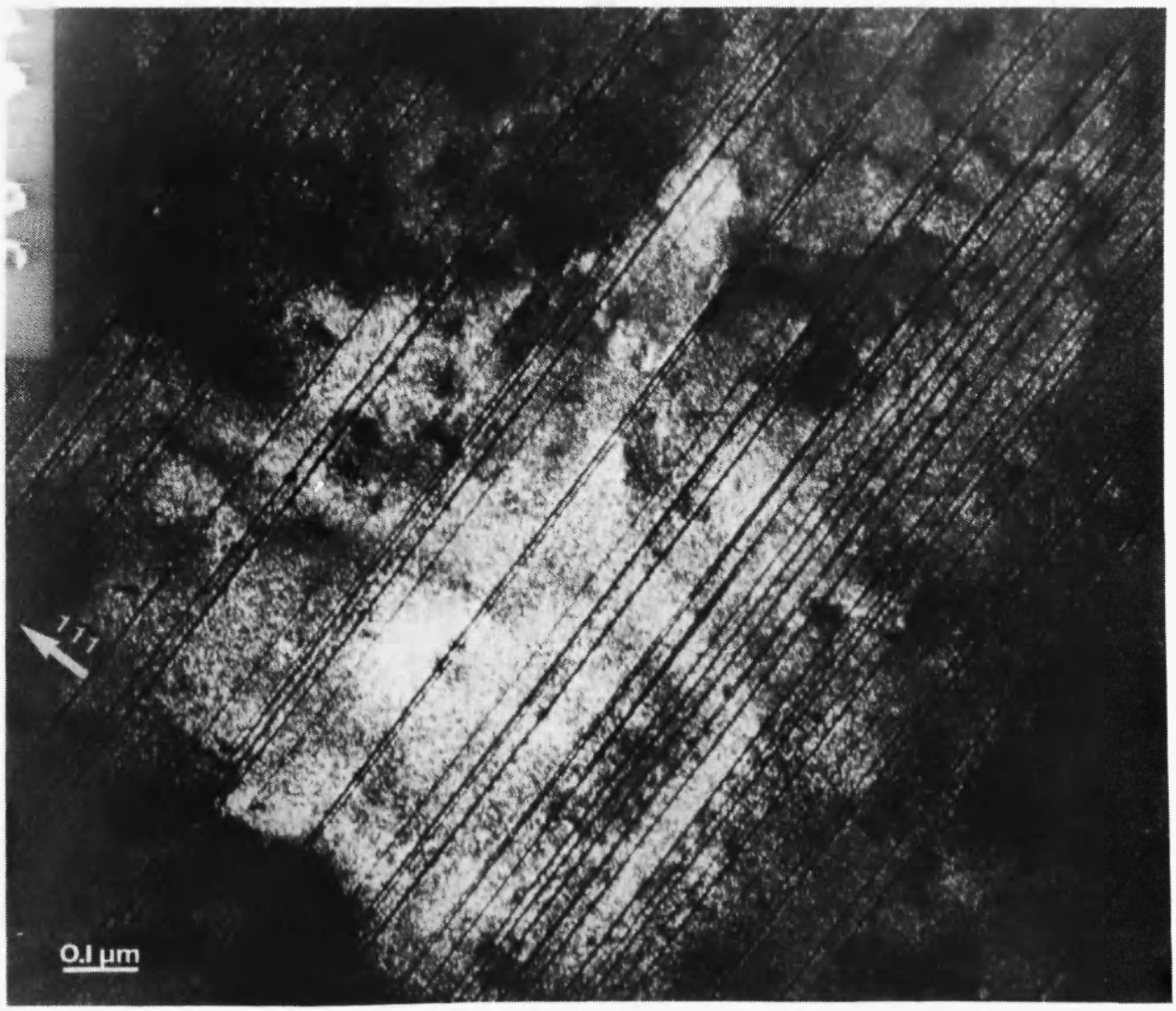

Fig. 8 : Al 2.5 % Li alloys : aged 8 h at 100°C fatigued ($\Delta\varepsilon_t$ = 0.3 %) : dissolution of δ' precipitates inside bands obtained during fatigue testing (superlattice dark field)

REFERENCES

(1) J.W. Martin "Micromechanisms in particle hardened alloys". Cambridge univ. press.
(2) V. Gerold, H.P. Karnthaler, Acta Met. 37, 2177 (1989).
(3) L.P. Kubin, Ph. Spiesser, Y. Estrin, Acta Met. 30, 385 (1982).
(4) D. Walgraef, E. Aifantis, J. Appl. Phys. 58. 2 (1985).
(5) Y. Brechet, F. Louchet in "nonlinear phenomena in material sciences" Aussois 1987 L.P. Kubin, G. Martin ed. p.347.
(6) C. Schiller, Thesis Univ. Bruxelles 1989.
(7) L.M. Brown, R. Ham in strengthening methods in solids Kelley Nicholson ed, p.9
(8) P. Guyot, Phil. Mag; 24, 989 (1971).
(9) B. Reppich, Acta Met., 23, 1055 (1975).
(10) Cavalieri "geometria indivisibilorum" 1635
(11) I.M. Lifschitz, V.V. Slyosov, J. Phys. Chem. Solids, 19, 35 (1961).
(12) P. Voorhees, J. Stat. Phys. 38, 1, 231 (1985).
(13) H. Mecking, Y. Estrin, Scripta. Met. 14, 815 (1980).
(14) P. Ortoleva, Z. Phys. B49, 149 (1982).
(15) S. Kai, S.C. Müller, Science on Forms 1, 9 (1985).
(16) J. loos, D. Joseph "Elementary stability and bifurcation theory" Springer verlag (1980).
(17) Y. Brechet, F. Louchet, C. Marchionni, J.L. Verger-Gaugry, Phil. Mag.A, 56, 353 (1987).
(18) J.W. Christian "The theory of transformations in metals and alloys" Pergamon (1965).
(19) J.W. Cahn, J. Hilliard, J. Chem. Phys., 28, 258 (1958).
(20) J.W. Cahn, Acta Met., 9, 795 (1961).
(21) J.W. Cahn, Acta Met., 9, 525 (1961).
(22) J.D. Gunton, M. San Miguel, P.S. Sahni in "Phase transitions and critical phenomena" C. Domb J.H. Lebowitz ed. Vol.8.

APPENDIX

List of symbols

σ : stress
σc : critical stress for precipitate overcoming
R : average radius of the intersection of the precipitate by the slip planes.
ℓ : precipitate separation in the slip plane
γ : antiphase boundary energy
b : Burgers vector modulus
Γ : line tension of dislocations
f : volume fraction of precipitates
ε : strain
$\dot{\varepsilon}$: strain rate
v : dislocation velocity
ρ : dislocation density
$\langle R \rangle$: average radius of precipitates
K : defined by eq. (8)
D : diffusion coefficient of solute atoms
γ_s : interfacial energy
Ω : atomic volume
c : solid solution concentration
k : Boltzmann constant
T : absolute temperature
D_o, α : constants defined by eq. (13)
L : distance between precipitates
c_p : solute concentration in precipitates
c_∞ : solute concentration in solid solution (read on the phase diagram)
β : $\frac{27}{8}K$
x : distance
q : instability wave vector
q_c : critical wave vector separating stable and unstable perturbations
n : number of precipitates per unit volume
γ_v : gain of bulk energy per unit volume during precipitation
R_c : critical radius for precipitate redissolution
R_{co} : critical radius of redissolution at zero strain
θ : characteristic time for precipitate dissolution
ξ : defined by eq. (27)
ΔG^* : saddle point energy for precipitation
γ_o : defined by eq. (32)
G : free enthalpy
c_o : nominal concentration
n_c : defined by eq. (35)
φ : defined by eq. (39)